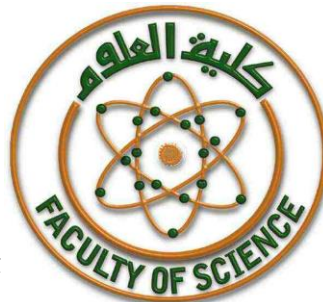




**Ain Shams University
Faculty of Science
Chemistry Department**



**Nanotechnology Open a New Era for the Evolution in Gas
Sensors “Nano-composite Materials as Dissolved Oxygen
Sensors”**

Ph.D. Thesis

Submitted To

**Chemistry Department - Faculty of Science - Ain Shams
University for the degree of Doctor Philosophy (Ph.D.) in
Science (Chemistry)**

By

Khaled Elsayed Mostafa Elsayed

Supervisors

Prof. Sayed Sabet Abd El Rehim

Prof. of Physical Chemistry- Faculty of Science-Ain Shams
University

Prof. Zeinab Abdel Hamid Abdel Aziz

Prof. of Physical Chemistry- Central Metallurgical Research &
Development Institute (CMRDI)

Prof. Taher Ahmed Salah Eldin

Prof. of Nanotechnology - Agricultural Research Center (ARC)

2021

Contents

| | |
|---|-----------|
| 1. Literature Review..... | 1 |
| 1.1 General introduction | 1 |
| 1.2 Electrochemistry and its application | 3 |
| 1.2.1 Oxidation-reduction reaction (ORR)..... | 3 |
| 1.3 The application of electrochemistry in the industry..... | 3 |
| 1.3.1 Sensors | 3 |
| 1.3.2 Classification of chemical sensors | 5 |
| 1.4 Electrochemical sensors | 6 |
| 1.5 Types of electrochemical sensors..... | 7 |
| 1.5.1 Potentiometric sensors..... | 7 |
| 1.5.2 Conductometric sensors | 8 |
| 1.5.3 Voltammetric/Amperometric sensors..... | 9 |
| 1.6 Types of Electrodes..... | 11 |
| 1.6.1 Reference electrode..... | 11 |
| 1.6.2 Counter Electrode..... | 12 |
| 1.6.3 Working Electrode..... | 12 |
| 1.6.4 Modified electrodes..... | 16 |
| 1.7 Nanotechnology in Electrochemical Sensors..... | 16 |
| 1.7.1 Nanomaterials (Types and Classification)..... | 17 |
| 1.7.2 Synthesis of nanoparticles..... | 19 |
| 1.8 A Brief Review on Nanomaterial Based Electrochemical Sensors | 23 |

| | | |
|-------|--|----|
| 1.9 | Dissolved oxygen sensor..... | 37 |
| 1.10 | Scope of the present investigation..... | 40 |
| 2. | Experimental Work and Techniques..... | 41 |
| 2.1 | Chemicals..... | 41 |
| 2.2 | Preparation of the nanomaterials..... | 41 |
| 2.2.1 | Preparation of graphene- Titanium dioxide (G-TiO ₂)..... | 41 |
| 2.2.2 | Preparation of Graphene-Titanium dioxide-Silver (G-TiO ₂ -Ag) | 43 |
| 2.2.3 | Electrochemical process and electrode preparation..... | 44 |
| 2.3 | Characterization techniques..... | 44 |
| 2.3.1 | X-Ray diffraction (XRD)..... | 44 |
| 2.3.2 | High Resolution Transmission Electron Microscope (HRTEM). | 46 |
| 2.3.3 | Field Emission Scanning Electron Microscope (FESEM)..... | 49 |
| 2.3.4 | Energy dispersive X-ray (EDX) system..... | 52 |
| 2.3.5 | Fourier Transform Infrared Spectroscopy (FTIR) Analysis..... | 53 |
| 2.4 | The Electrochemical sensor performance test..... | 53 |
| 3. | Results and Discussion..... | 55 |
| 3.1 | Nanomaterial Characterization..... | 55 |
| 3.1.1 | X-Ray diffraction..... | 55 |
| 3.1.2 | High Resolution Transmission Electron Microscope (HRTEM)... | 57 |
| 3.1.3 | Fourier Transform Infrared Spectroscopy (FTIR)..... | 62 |
| 3.2 | Surface characterization of the modified electrodes..... | 64 |
| 3.2.1 | Field emission scanning electron microscope (FESEM)..... | 64 |
| 3.2.2 | Energy dispersive X-ray and mapping analysis..... | 69 |

| | | |
|--------------|---|------------|
| 3.3 | Electrochemical behavior of the prepared electrodes | 75 |
| 3.3.1 | Effect of electrode kind | 75 |
| 3.3.2 | Effect of dissolved oxygen (DO) concentration | 81 |
| 3.3.3 | Effect of scan rate | 84 |
| 3.4 | Amperometric study of the prepared modified electrodes | 89 |
| 3.4.1 | Electrodes sensitivity and detection limit | 92 |
| 3.4.2 | Active material loading concentration effect on the sensitivity... | 98 |
| 4. | Conclusion..... | 104 |
| 5. | References | 106 |

List of Figures

| | |
|--|-----------|
| <i>Figure 1: Different classes of chemical sensors.....</i> | <i>5</i> |
| <i>Figure 2: Schematic representation of a typical voltammetric sensing system.</i> | <i>7</i> |
| <i>Figure 3: Classes of carbon-based nanoparticles: (i) Fullerenes, (ii) Graphene, (iii) Carbon nanotubes, (iv) Carbon nanofibers and (v) Carbon black [83].....</i> | <i>18</i> |
| <i>Figure 4: Organic nanoparticles include (i) Dendrimers, (ii) Liposomes and (iii) micelles [85].....</i> | <i>18</i> |
| <i>Figure 5: Approaches for nanoparticle synthesis.</i> | <i>20</i> |
| <i>Figure 6: Green synthesis of nanoparticles by different biological sources.</i> | <i>23</i> |
| <i>Figure 7: Schematic diagram of the preparation steps for G-TiO₂ nanocomposite.</i> | <i>42</i> |
| <i>Figure 8: Schematic diagram of the preparation steps for G-TiO₂-Ag nanocomposite</i> | <i>43</i> |
| <i>Figure 9: X-ray diffraction (XRD) (X'Pert PRO – PANalytical, Netherlands).....</i> | <i>45</i> |
| <i>Figure 10: Difference in the internal structure of LM and TEM</i> | <i>47</i> |
| <i>Figure 11: High Resolution Transmission Electron Microscope (HR-TEM) (Tecnai, G₂-20 S-Twin - FEI, Netherland).....</i> | <i>48</i> |
| <i>Figure 12: Schematic diagram of the components of SEM.....</i> | <i>49</i> |
| <i>Figure 13: types of the electron source.....</i> | <i>50</i> |
| <i>Figure 14: Schematic for electron beam interaction</i> | <i>51</i> |
| <i>Figure 15: Field Emission Scanning Electron Microscope (FESEM) Quattro S, Thermo Fischer scientific, US.</i> | <i>52</i> |

| | |
|--|----|
| <i>Figure 16: FTIR, Bruker vertex 70</i> | 53 |
| <i>Figure 17: XRD pattern for Graphene (G) nanosheets</i> | 55 |
| <i>Figure 18: XRD pattern for Graphene – Titanium dioxide (G-TiO₂) nanosheets</i> | 56 |
| <i>Figure 19: XRD pattern for Titanium dioxide-nanosilver (TiO₂-Ag)</i> | 57 |
| <i>Figure 20: XRD pattern for Graphene-Titanium dioxide-nano silver (G-TiO₂-Ag)</i> | 57 |
| <i>Figure 21: TEM image for Graphene (G) sheet</i> | 58 |
| <i>Figure 22: TEM image for G-TiO₂ nanocomposite, Inset image is for SAED.</i> | 59 |
| <i>Figure 23: TEM image for TiO₂ – Ag nanocomposite, Inset image is for SAED.</i> | 60 |
| <i>Figure 24: High resolution TEM image for TiO₂-Ag nanocomposite showing the lattice spacing for TiO₂ and Ag nanoparticles.</i> | 61 |
| <i>Figure 25: TEM image for G-TiO₂ -Ag nanocomposite, inset image is for SAED.</i> | 62 |
| <i>Figure 26: FTIR spectrum for; G, G-TiO₂, TiO₂-Ag and G-TiO₂-Ag</i> | 63 |
| <i>Figure 27: FESEM image for bare glassy carbon electrode (GCE) surface.</i> | 64 |
| <i>Figure 28: FESEM image for modified GCE with graphene (G) (GCE/G).</i> | 65 |
| <i>Figure 29: FESEM image for modified GCE with G-TiO₂.</i> | 65 |
| <i>Figure 30: FESEM image for modified GCE with TiO₂-Ag</i> | 66 |
| <i>Figure 31: FESEM image for modified GCE with G-TiO₂-Ag.</i> | 66 |
| <i>Figure 32: High magnification FESEM image for G/GC modified electrode</i> | 67 |

| | |
|---|----|
| <i>Figure 33: High magnification FESEM image for G-TiO₂/GC modified electrode.</i> | 68 |
| <i>Figure 34: High magnification FESEM image for TiO₂-Ag/GC modified electrode.</i> | 68 |
| <i>Figure 35: High magnification FESEM image for G-TiO₂-Ag/GC modified electrode.</i> | 69 |
| <i>Figure 36: EDX analysis for Glassy carbon (GC)/ graphene (G) electrode.</i> | 70 |
| <i>Figure 37: EDX analysis for GC/ TiO₂-Ag electrode.</i> | 70 |
| <i>Figure 38: EDX analysis for GC/ G-TiO₂ and GC/ G-TiO₂-Ag electrode.</i> | 71 |
| <i>Figure 39: Mapping for GC/G electrode surface shows distribution of a) Carbon, b) Oxygen and c) Fluorine element.</i> | 72 |
| <i>Figure 40: Mapping for GC/TiO₂-Ag electrode surface shows distribution of a) Carbon, b) Oxygen, c) Fluorine, d) Ti and e) Ag element.</i> | 73 |
| <i>Figure 41: Mapping for GC/G-TiO₂ electrode surface shows distribution of a) Carbon, b) Oxygen, c) Fluorine, d) Ti element.</i> | 74 |
| <i>Figure 42: Mapping for GC/G-TiO₂-Ag electrode surface shows distribution of a) Carbon, b) Oxygen, c) Fluorine, d) Ti and e) Ag element.</i> | 75 |
| <i>Figure 43: Cyclic voltammetry for the bare GC electrode in PBS pH 7.0, a) N₂-saturated and b) O₂-saturated.</i> | 77 |
| <i>Figure 44: Cyclic voltammetry for the GC/G electrode in PBS pH 7.0, a) N₂-saturated and b) O₂-saturated.</i> | 78 |
| <i>Figure 45: Cyclic voltammetry for the GC/TiO₂-Ag electrode in PBS pH 7.0, a) N₂-saturated and b) O₂-saturated.</i> | 79 |
| <i>Figure 46: Cyclic voltammetry for the GC/G-TiO₂ electrode in PBS pH 7.0, a) N₂-saturated and b) O₂-saturated.</i> | 80 |

Figure 47: Cyclic voltammetry for the GC/G-TiO₂-Ag electrode in PBS pH 7.0, a) N₂-saturated and b) O₂-saturated. 81

Figure 48: Cyclic voltammetry for GC/G modified electrode in PBS (pH 7) for different DO concentrations (from 1 to 30 μM). 82

Figure 49: Cyclic voltammetry for GC/ TiO₂-Ag modified electrode in PBS (pH 7) for different DO concentrations (from 1 to 30 μM). 82

Figure 50: Cyclic voltammetry for GC/ G-TiO₂ modified electrode in PBS (pH 7) for different DO concentrations (from 1 to 30 μM). 83

Figure 51: Cyclic voltammetry for GC/ G-TiO₂-Ag modified electrode in PBS (pH 7) for different DO concentrations (from 1 to 30 μM). 83

Figure 52: Relation between the reduction peak current of DO at various concentrations in PBS (pH 7) at 50 mV s⁻¹ at: a) GC/G-TiO₂ and b) GC/G-TiO₂-Ag electrode. 84

Figure 53: a) Cyclic voltammetry for GC/G modified electrode in PBS (pH 7) O₂ - saturated at different scan rates/ (10, 30, 50, 80, 100 and 120 mV s⁻¹). b) The linear relation between the peak current with the square root of scan rate. 85

Figure 54: a) Cyclic voltammetry for GC/TiO₂-Ag modified electrode in PBS (pH 7) O₂ - saturated at different scan rates/ (10, 30, 50, 80, 100 and 120 mV s⁻¹). b) The linear relation between the peak current with the square root of scan rate. 86

Figure 55: a) Cyclic voltammetry for GC/G-TiO₂ modified electrode in PBS (pH 7) O₂ - saturated at different scan rates/ (10, 30, 50, 80, 100 and 120 mV s⁻¹). b) The linear relation between the peak current with the square root of scan rate. 87

Figure 56: a) Cyclic voltammetry for GC/G-TiO₂-Ag modified electrode in PBS (pH 7) O₂ - saturated at different scan rates/ (10, 30, 50, 80, 100 and 120 mV s⁻¹). b) The linear relation between the peak current with the square root of scan rate. 88

Figure 57: Amperometric response for the dissolved oxygen reduction on GC/G modified electrode in PBS (pH 7) for concentrations of; 1, 4, 8, 12, 16, 20, 25, 30, 40, 50, 60, 70, 80, 100 μ M. Applied potential: -300 mV..... 89

Figure 58: Amperometric response for the dissolved oxygen reduction on GC/TiO₂-Ag modified electrode in PBS (pH 7) for concentrations of; 1, 4, 8, 12, 16, 20, 25, 30, 40, 50, 60, 70, 80, 100 μ M. Applied potential: -300 mV. 90

Figure 59: Amperometric response for the dissolved oxygen reduction on GC/G-TiO₂ modified electrode in PBS (pH 7) for concentrations of; 1, 4, 8, 12, 16, 20, 25, 30, 40, 50, 60, 70, 80, 100 μ M. Applied potential: -300 mV. 91

Figure 60: Amperometric response for the dissolved oxygen reduction on GC/G-TiO₂-Ag modified electrode in PBS (pH 7) for concentrations of; 1, 4, 8, 12, 16, 20, 25, 30, 40, 50, 60, 70, 80, 100 μ M. Applied potential: -300 mV. 92

Figure 61: The calibration curve for GC/G modified electrode. 94

Figure 62: The calibration curve for GC/G-TiO₂ modified electrode. 95

Figure 63: The calibration curve for GC/ TiO₂-Ag modified electrode. 96

Figure 64: The calibration curve for GC/G-TiO₂-Ag modified electrode.. 97

Figure 65: Effect of different concentrations of G in GC/G modified electrode on the sensitivity..... 99

Figure 66: Effect of different concentrations of G-TiO₂ in GC/G-TiO₂ modified electrode on the sensitivity. 99

Figure 67: Effect of different concentrations of TiO₂ – Ag in GC/ TiO₂-Ag modified electrode on the sensitivity. 100

Figure 68: Effect of different concentrations of G -TiO₂ - Ag in GC/ G-TiO₂-Ag modified electrode on the sensitivity..... 101

Figure 69: Chronoamperometry of G-TiO₂ and G-TiO₂-Ag electrodes at -400 mV (SCE) in O₂-saturated 0.1 M PBS. 103

List of Tables

| | |
|--|-----------|
| <i>Table 1: Advantages and disadvantages of electrochemical sensors</i> | <i>11</i> |
| <i>Table 2: Chemicals used in the study.</i> | <i>41</i> |
| <i>Table 3: Comparison between light microscope (LM) and electron microscope (EM).....</i> | <i>46</i> |

List of Abbreviations

| Word | Abbreviations |
|---|---------------|
| Zero-Dimensional | 0D |
| One-Dimensional | 1D |
| Two-Dimensional | 2D |
| Anodic Stripping Voltammetry | ASV |
| Poly(bromocresol green) | BCG |
| Backscattered Detector | BSD |
| Counter Electrode | CE |
| Carbon Nanotube | CNT |
| Carbon Paste Electrode | CPE |
| Cathodic Stripping Voltammetry | CSV |
| Cyclic Voltammetry | CV |
| Chemical Vapor Deposition | CVD |
| Coated Wire Electrodes | CWES |
| Dopamine | DA |
| Dropping Mercury Electrode | DME |
| Dissolving Oxygen | DO |
| Differential Pulse Voltammetry | DPV |
| Energy Dispersive Spectroscopy | EDS |
| Energy Dispersive X-ray | EDX |
| Electrodeposited Graphene | EGR |
| Fetal Bovine Serum | FBS |
| Field Emission Scanning Electrone Microscope | FESEM |
| Field Effect Transistors | FETS |
| Fourier Transform Infrared Spectroscopy | FTIR |
| Fluorine-doped Tin Oxide | FTO |
| Graphene | G |
| Glassy Carbon | GC |
| Glassy Carbon Electrode | GCE |
| Graphene Nanosheet | GNS |
| Graphene Oxide | GO |
| Hanging Mercury Drop Electrode | HMDE |
| High Resolution Transmission Electron Microscope | HRTEM |

| | |
|--|----------|
| International Center for Diffraction Data | ICDD |
| Infra-Red | IR |
| Ion Selective Electrode | ISE |
| Indium- Tin Oxide | ITO |
| Light Microscope | LM |
| Linear Sweep Voltammetry | LSV |
| Magnetic Bar Carbon Paste Electrode | MBCPE |
| Mercury Film Electrode | MFE |
| Molecularly Imprinted Star Polymers | MISP |
| Mercury-Mercury Oxide | MMO |
| Mercury-Mercurous Sulfate | MMS |
| Multi-Walled Carbon Nanotube | MWCNT |
| Nanoparticles | NPs |
| Normal Pulse Voltammetry | NPV |
| Organic Electrochemical Transistor | OECT |
| Organophosphate Compounds | OPs |
| Oxygen Reduction Reaction | ORR |
| Phosphate Buffer Solution | PBS |
| Reference Electrode | RE |
| Reduced Graphene Oxide | rGO, RGO |
| Reversible Hydrogen Electrode | RHE |
| Rizatriptan Benzoate | RZB |
| Selected Area Electron Diffraction | SAED |
| Saturated Calomel Reference Electrode | SCE |
| Secondary Electron Detector | SED |
| Standard Hydrogen Electrode | SHE |
| Silver-Silver Chloride Electrode | SSCE |
| Silver-Silver Sulfate Electrode | SSSE |
| Square Wave Voltammetry | SWV |
| Tetraethoxysilane | TEOS |
| Tetramethoxysilane | TMOS |
| Titanium (IV) Isopropoxide | TTIP |
| Working Electrode | WE |
| X-Ray Diffraction | XRD |

Summary

The determination of dissolved oxygen (DO) is an important parameter for the indication of water quality for aquaculture farming and for various physiological and biochemical parameters, such as the monitoring of DO in cell culture and in vivo study is considered to be one of the most important requirements. This study is focused on tailoring an efficient nano-sized catalyst for DO sensing with high sensitivity and low detection limit to substitute the highly cost Pt catalyst and minimize the overpotential of oxygen reduction reaction (ORR).

In the thesis, the first chapter introduces a general introduction followed by literature review about the electrochemical sensors and their impacts in detection of many species. A review of the researches that had been done to develop such sensors using nanomaterials and their applications as dissolved oxygen (DO) sensors. Then the second chapter shows the methodology of the experiments, the fabrication techniques and the chemicals in addition to the characterization techniques. The last chapter reviews the results that have been reached and their interpretation.

The hydrothermal methods was used to prepare Graphene (G) nanosheets, Graphene- titanium dioxide (G-TiO₂), titanium dioxide –silver (TiO₂-Ag) and Graphene-titanium dioxide-silver (G-TiO₂-Ag) nanocomposites. The formation and the shape of the prepared nanomaterials were confirmed using X-ray diffraction (XRD), fourier-transform infrared spectroscopy (FTIR) and High resolution transmission electron microscope (HRTEM) and all results were discussed.

Glassy carbon electrode surface was cleaned and polished well then modified with the prepared nanocomposites each composite for one electrode. Field emission scanning electron microscope (FESEM) was used

to study the modified electrode surface morphology and confirm the presence and distribution of the nanomaterials on the electrode surface using energy dispersive X-ray (EDX) and mapping analysis techniques. The results showed the presence and the good distribution of the nanomaterials on the electrode surface.

The electrochemical behavior for the prepared electrodes toward the dissolved oxygen (DO) using the cyclic voltammetry technique (CV) was performed. The results showed that the highest response in DO saturated solution was for the electrode modified with G-TiO₂-Ag.

The response for the different concentrations of DO in the solution was varied according to the sensitivity for each electrode but was also matched with the results in case of saturated oxygen solution. The sensitivity and the detection limit for each electrode were evaluated using the amperometric technique.

The sensitivity for glassy carbon electrodes (GC) / G-TiO₂-Ag and GC/TiO₂-Ag was 1.363 $\mu\text{Acm}^{-2}\mu\text{M}^{-1}$ and 1.3034 $\mu\text{Acm}^{-2}\mu\text{M}^{-1}$, respectively. The detection limit (LOD) also was the best for the previous electrodes with detection limit of 0.011 μM for GC/G-TiO₂-Ag and detection limit of 0.022 μM for GC/TiO₂-Ag.

Material loading concentration factor indicated that 15 mg of the loaded material leads to better sensitivity for all materials examined but 20 mg decreases the sensitivity but still higher than that for 10 mg in case of G-TiO₂-Ag, except in case of TiO₂-Ag the sensitivity decreased at loading concentration of 25 mg and still higher than that for 10 mg.